

Climate Change and Arctic Infrastructure

Arne Instanes

Instanes Svalbard AS, N-9171 Longyearbyen, NORWAY, e-mail: arne.instanes@opticonsult.no

Oleg Anisimov

State Hydrological Institute, St. Petersburg, RUSSIA, e-mail: oleg@oa7661.spb.edu

Abstract

Several authors report that impacts of climate change on infrastructure in the Arctic are already evident. Damage to infrastructure and engineering structures in permafrost regions are often linked to observed increase in air temperature over the last 10 to 20 years. However, these reports do not show in detail how the change in air temperature may affect the active layer thickness and permafrost temperature at specific sites and for specific structures in the Arctic.

This paper presents the results of a study of the impact of climate change on Arctic infrastructure based on historical meteorological records. The temperature data are used together with a numerical model to evaluate the possible warming of permafrost at depth, and theoretical impacts on pile foundation capacity at specific sites in the Arctic. Results from permafrost model forced by several GCM-based climatic projections are used to construct the predictive map indicating threats to infrastructure due to potential weakening of the frozen ground.

Keywords: Climate change; Engineering; Foundations; Geotechnical; Permafrost; Warming.

Introduction

Modern and projected for the future climatic changes are more pronounced in the Arctic than in many other parts of the world. For several decades, air temperatures in the Arctic have warmed at approximately twice the global rate (McBean *et al.*, 2005). Zonal-mean temperature north of 60°N has increased up to 2 °C since late 1960s. Contemporary warming in the Arctic is strongest (~ 1 °C/decade) in winter and spring, and smallest in autumn. Such changes lead to warming, thawing, and degradation of permafrost. Observational data are limited, and are not available throughout the entire Arctic. Borehole measurements indicate that permafrost temperatures have increased markedly during the last 50 years, (Romanovsky *et al.*, 2002), with rapid warming in Alaska (Hinzman *et al.*, 2005), Canada (Beilman *et al.*, 2001), Europe (Harris *et al.*, 2003), and Siberia (Pavlov and Moskalenko, 2002).

In the context of the future climate change one of the key concerns associated with the thawing of permafrost is the detrimental impact on the infrastructure built upon it. Several authors report that such impacts are already evident (Khrustalev, 2001; Romanovsky and Osterkamp, 2001; Zernova, 2003; Gribchatov, 2004; Vasilieva, 2004). Instanes *et al.* (2005) and Instanes (2003) conclude that human interaction and engineering construction very often leads to extensive thawing of both continuous and discontinuous permafrost even if the climatic conditions remain unchanged. The intergovernmental panel on climate change (Anisimov and Vaughan, 2007) also points out that the effect of heated buildings on underlying ice-rich permafrost has been known for a very long time and may be mistaken for an impact of climate change.

In this paper we used historical air temperature records from three different cities to investigate the change in pile foundation bearing capacity during the last 100 years. We

upscaled the results of this historical analysis and constructed the map of potential threats to infrastructure using the hazard index that takes into account regionality of projected climatic and permafrost changes.

Pile design

Design ground temperature

The strength and deformation characteristics of frozen soils are temperature dependent. It is, therefore, necessary to determine the thickness of the active layer (maximum thaw depth) and the maximum ground temperature along the embedded pile length (Andersland and Ladanyi, 2004). These two parameters are incorporated into the site-specific design of foundations in permafrost regions. Conventional engineering design is based on the analysis of historical variations of climatic and permafrost data and accounts for the frequency of extreme events, such as abnormally high temperatures resulting in deeper seasonal thawing of permafrost. Each foundation is designed with construction-specific safety factor that depends on the probability of such extremes.

Adfreeze bonds

The adfreeze bond strength between the pile surface and surrounding frozen permafrost soil is temperature and time dependent. For a specific pile foundation design, this parameter should be determined from geotechnical field and laboratory investigations. For the purpose of this study a simplified relationship is used as shown in Figure 1.

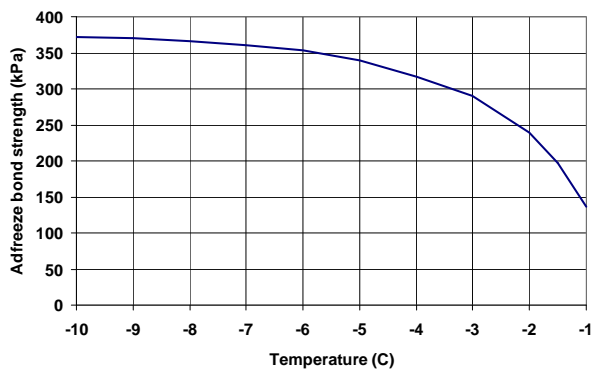


Figure 1 Adfreeze bond strength used in the analysis

Data in Figure 1 may be used to evaluate the effect of changing climatic conditions on the bearing capacity of piles and thus to predict the potentially detrimental impacts of warming and thawing permafrost on the structures built upon it.

Air temperature records

The climatic data used in the present analysis were mean monthly air temperatures from three different locations in the Arctic: i) Fairbanks, Alaska (N64°15', W147°37'), ii) Longyearbyen, Norway (N78°25', E15°47') and iii) Yakutsk, Russia (N62°02', E129°45'). The sites were chosen based on:

- station time series approximately 100 years or more,
- location near population concentrations and major infrastructure,
- locations representing different climatic and environmental conditions in the Arctic.

All three stations show some indication of increased air temperatures during the last 20 to 30 years. Yakutsk has the longest time series starting in 1829, while the time series for Fairbanks and Longyearbyen start in 1904 and 1912, respectively.

Figure 2 shows mean annual air temperatures for Yakutsk, Longyearbyen, and Fairbanks smoothed with 30-years running filter. In the last three to four decades temperatures increased by almost 2 °C in Yakutsk, and by 1 °C in Fairbanks, see Figure 2. In Longyearbyen there was the decrease of the annual mean air temperature from the maximum of -5.2 °C in 1960 to the minimum of -6.8 °C in 1990 followed by rapid increase by ca. 1 °C since then. Based on Figure 2, the temperatures in the 1960s was still higher than now. However, Longyearbyen had a mean annual air temperature in 2006 that was the warmest recorded (-1.6 °C).

We used these data in the thermal model to calculate the changes in the ground temperature at different depth and to evaluate the effect it had on the bearing capacity of piles.

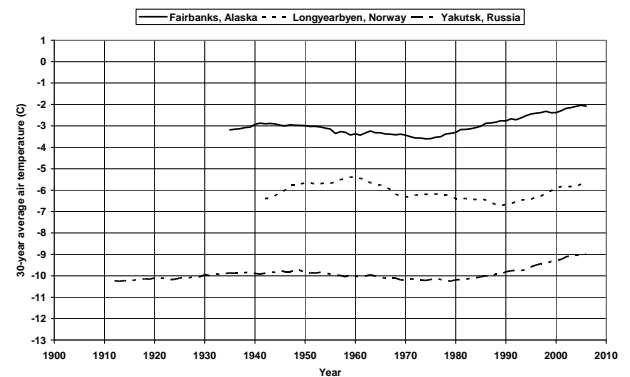


Figure 2. Mean annual air temperatures for Fairbanks, Alaska; Longyearbyen, Norway and Yakutsk, Russia, smoothed with 30-years running filter.

Thermal model and results

The thermal model used in the analyses was TEMP/W, version 7.03 (Geo-Slope, 2007). TEMP/W is a finite element software that can model the thermal changes in the ground due to changing temperature or heat flux boundary conditions. It also accounts for the effects of the temperature dependent thermal conductivity, volumetric latent heat of fusion, and soil unfrozen water content. In this study we used a simplified homogenous soil profile consisting of silty sand with the following parameters:

- dry density (γ_d): 16.7 kN/m³ ($\rho_d=1700$ kg/m³),
- water content (w): 20%,
- degree of saturation (S_r): 100%
- porosity (n): 37.1%,
- volumetric heat capacity frozen (c_{vu}): 2300 kJ/(m³K),
- vol. heat capacity unfrozen (c_{vu}): 3150 kJ/(m³K).

Thermal conductivity and heat capacity was adjusted to changing ground temperature and unfrozen water content using simplified empirical relationships.

The soil profile was modeled using isoparametric 8-nodes quadrilateral finite elements. Mean monthly air temperatures were applied to the surface boundary of the finite element mesh. The initial ground temperature at the start of the analyses (1904 for Fairbanks, 1912 for Longyearbyen and 1900 for Yakutsk) was set approximately equal to the mean annual air temperature in Figure 2.

It should be noted that n-factors of 1.0 was used in the analysis presented in this paper. Andersland and Ladanyi (2004) suggest that n-factors between 1.2 and 2.0 would be appropriate for sand and gravel surfaces during thawing.

The ultimate goal of the calculations was to evaluate the probability for the ground temperature to exceed the threshold beyond which the pile becomes unstable and is not capable to bear the load of construction above it. Figures 3-5 present the maximum ground temperatures along the embedded pile length for selected years for Fairbanks, Longyearbyen and Yakutsk, respectively. Maximum ground temperatures for each decade is presented in Tables 1, 2 and 3. It can be observed from the figures and tables that all three locations have the highest ground temperatures after year 2000.

Computed and measured ground temperatures are in good agreement in Longyearbyen. For Fairbanks and Yakutsk the computed values seem to be lower than observed ground temperatures. This is probably due to the effect of the n-factor used in the analysis, see above. The thermal model should, therefore, be tuned with actual ground temperature observations. However, the main purpose of the study was to look at the relative effect of variations in air temperatures over the last 100 years for an idealized soil profile and the results show that this goal has been achieved.

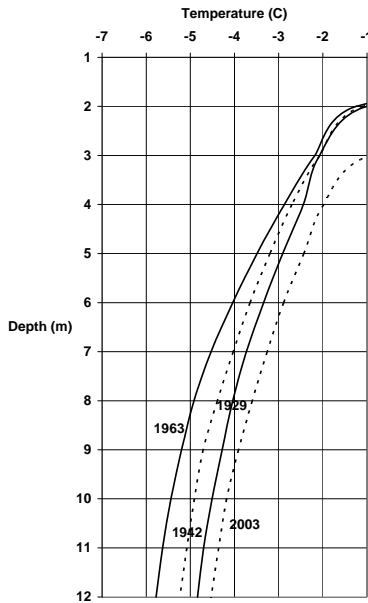


Figure 3 Maximum ground temperature along the embedded pile length, Fairbanks 1929, 1942, 1963 and 2003.

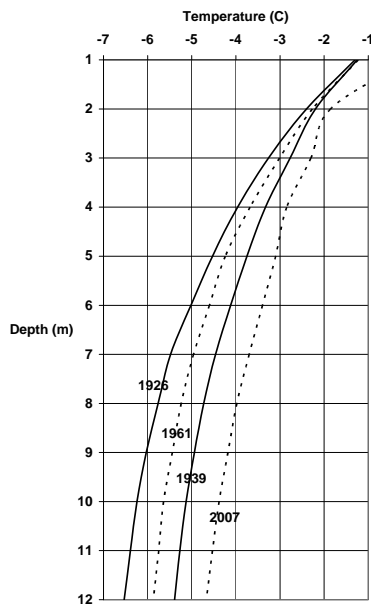


Figure 4 Maximum ground temperature along the embedded pile length, Longyearbyen 1926, 1939, 1961 and 2007.

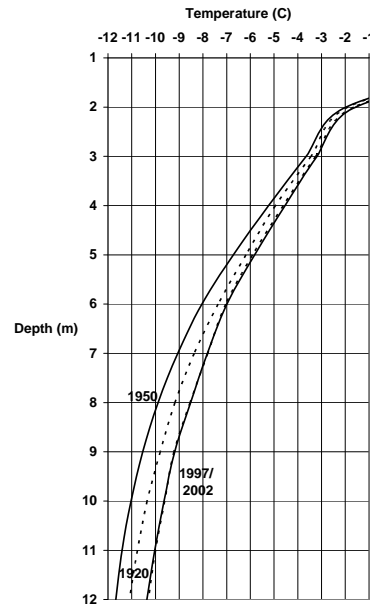


Figure 5 Maximum ground temperature along the embedded pile length, Yakutsk 1920, 1950 and 1997/2002.

Pile capacity

Based on the maximum ground temperatures presented in Tables 1, 2 and 3 and the adfreeze bond strength presented in Figure 1, theoretical pile capacities for a 200 mm diameter pile for the three locations are presented in Figure 6. As follows from the figure, in Fairbanks the theoretical pile capacity has been reduced by 6.5% from 627 kN in 1963 to 587 kN in 2003. In Longyearbyen the pile capacity has been reduced by 12.5% from 717 kN in 1977 (and 1926) to 636 kN in 2007. In Yakutsk, the theoretical pile capacity has remained almost unchanged with only slight reduction by 1.5% in the period 1950-2002. This is because ground temperatures in Yakutsk are low (<-6 °C below 5 meters depth, see Table 3), while the adfreeze bond strength does not change much for temperatures below -5 to -6 °C (see Figure 1). Pile capacities in Longyearbyen are higher than in Yakutsk because the active layer thickness here is much smaller due to the relatively cold summers in Spitsbergen compared to central Yakutia. It implies that the embedded length of the pile that has a temperature below -1 °C (also called the effective pile length) is bigger in Longyearbyen (approximately 11 meters) than in Fairbanks and Yakutsk (approximately 10 m).

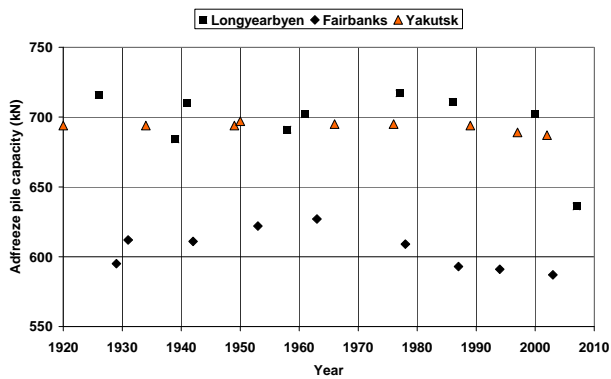


Figure 6 Theoretical adfreeze pile capacity for a 200 mm pile.

Hazard map

Results from the three selected sites indicate strong regionality of the impacts that climatic warming in the last few decades has had on the bearing capacity of pile foundations. Nelson *et al.* (2001) suggested the hazard index for predictive mapping of potential risks to infrastructure due to warming and thawing of permafrost. This index is constructed using combination of projected for the future changes in the depth of seasonal thawing and the ice content of the frozen ground. Changes in the ground temperature, although explicitly not included in the index, are taken into account in permafrost model that is used to calculate the projected thaw depth. The more recent study by Anisimov and Lavrov (2004) uses modified hazard index that also includes the salinity of soils, which is particularly important in the vicinity of the Arctic shoreline. In the geological past these areas were underneath the sea level, and salt has been deposited in the upper soil layer. Even slight temperature variation may shift the balance between the ground ice and unfrozen water in such soils, which are thus particularly sensitive to climatic changes. Modified hazard index, I_G , is given by the following equation:

$$I_G = \Delta Z_{al} V_{ice} K_s \quad (1)$$

Here ΔZ_{al} is the projected change in the depth of seasonal thawing, expressed in relative units with respect to modern norm; V_{ice} is the volumetric ground ice content, and K_s is the coefficient that characterizes soil salinity.

Hazard index for Russian permafrost regions has been calculated using results from permafrost model forced by several climatic scenarios. The mathematical formalism has been detailed in several preceding publications, *i.e.* (Anisimov *et al.*, 2007; Sazonova and Romanovsky, 2003). All calculations were made in the nodes of 0.5° lat/long grid spanning the northern Eurasian permafrost region.

The model was forced by the contemporary and projected for the future climatic data. We used gridded monthly norms of air temperature and precipitation with 0.5° lat/long resolution as baseline data characterizing modern climate (New *et al.*, 1999). Set of five scenarios of climate change

for the 11-year long time periods centred on 2030, 2050, and 2080 has been constructed by superimposing predicted by CGCM2, CSM_1.4, ECHAM4/OPYC3, GFDL-R30_c and HadCM3 GCMs changes of climatic parameters on baseline data. These GCMs were selected as a result of the survey made in the course of the ACIA (Arctic Climate Impact Assessment) because they account for many key processes in the Arctic and provide reasonable fit to the observed climatic trends (Symon, 2005). All climate models were forced by the B2 emission scenario. The climatic scenarios are fully documented in the ACIA report (2005) and are available on the web sites of the data distribution center of the Intergovernmental Panel on Climate Change (IPCC; <http://ipcc-ddc.cru.uea.ac.uk/> and <http://igloo.atmos.uiuc.edu/IPCC/>).

Soil thermal properties were calculated using parameterizations that take into account soil type, soil moisture and ground ice content. We calculated winter-average snow depth at each node using monthly precipitation data. The density, thermal conductivity, and heat capacity of snow were prescribed at 300 kg m^{-3} , $0.23 \text{ W m}^{-1} \text{ K}^{-1}$ and $2090 \text{ J kg}^{-1} \text{ K}^{-1}$, respectively. Vegetation types with prescribed thermal properties and soil type were obtained from the digital global ecosystems database (1992). The model was validated by the data from Circumpolar Active Layer Monitoring program (Brown *et al.*, 2000) and used to calculate permafrost parameters under modern and projected for the future climatic conditions. Results of such calculations differ in detail depending on climatic scenario. Predictive map of hazard index in Figure 7 was constructed using the “median” climatic projection of GFDL model for 2050

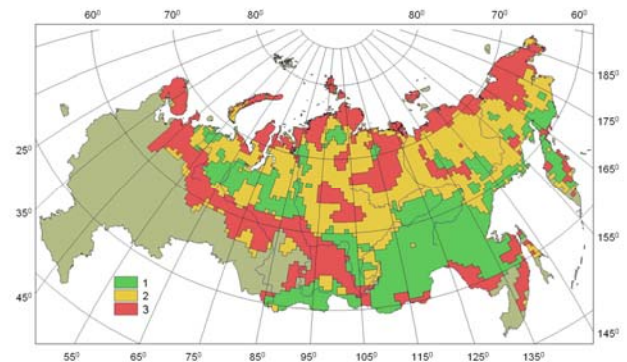


Figure 7. Predictive map of potential threats to infrastructure for 2050. Red, yellow and green colors designate regions with high, moderate, and low susceptibility of buildings and engineered structures to the ongoing climatic and permafrost changes.

Summary and Conclusions

Historical air temperature records indicate warming during the last few decades in three selected locations representing different climatic and environmental conditions

on Spitsbergen, in central Yakutia, and on Alaska. The results from this study suggest that piled foundations have not suffered sufficient loss in bearing capacity to become unstable due to the observed increase in air temperatures. However, the loss in capacity of piles in Longyearbyen from 702 kN to 636 kN in the period 2000-2007 is the early warning of the potentially detrimental impacts of changing climate.

One of the apparent features of the climate change impacts in permafrost regions is strong regionality. Susceptibility of permafrost to climatic changes and associated risks to infrastructure depend on the combinations of local soil, topographic, hydrological, vegetation, and snow conditions. In this paper the large-scale pattern of the future impacts was studied using the hazard index. Although such index provides highly generalized information about the potential impacts on the infrastructure, it may serve as effective tool for resource and land use planning, environmental risk management, and civil engineering in permafrost regions.

Areas of greatest hazard potential in Figure 7 include the Arctic coastline and parts of Siberia in which substantial development has occurred in recent decades. Particular concerns are associated with Yamal peninsula that falls into the highest risk zone, because of the ongoing expansion of the oil and gas extracting and transportation industry into this region. Although temperatures here are relatively low, frozen ground is already very unstable, largely because of its high salinity, and thus even small warming may cause extensive thawing of permafrost and ground settlement with serious impacts on the infrastructure.

Acknowledgements

Anisimov's research of the contemporary climatic changes in Russia and predictive modelling of the impacts of thawing permafrost on infrastructure is supported by the Russian Foundation for Basic Research, grants # 07-05-00209 and 07-05-13527.

References

- Andersland, O.B. and Ladanyi, B. 2004. *Frozen ground engineering*. 2nd edition. New Jersey, USA: John Wiley & Sons, Inc. Published in cooperation with ASCE press. 363 pages.
- Anisimov, O.A. and Lavrov, C.A., 2004. Global warming and permafrost degradation: risk assessment for the infrastructure of the oil and gas industry. *Technologies of oil and gas industry*, (3): 78-83 (in Russian).
- Anisimov, O.A. and D.G. Vaughan, 2007. Polar Regions. In: *Climate Change 2007: Climate change impacts, adaptation, and vulnerability. Contribution of Working group II to the Fourth Assessment Report of the Intergovernmental Panel on Climate Change*.
- Anisimov, O.A., Lobanov, V.A., Reneva, S.A., Shiklomanov, N.I., Zhang, T., 2007. *Uncertainties in gridded air temperature fields and their effect on predictive active layer modeling*. Journal of Geophysical Research, 112 (F02S14), doi:10.1029/2006JF000593/
- Beilman, D.W., D.H. Vitt, and L.A. Halsey, 2001: Localized permafrost Peatlands in Western Canada: Definition, distributions, and degradation. *Arct. Antarct. Alp. Res.*, 33(1), 70-77.
- Brown, J., Hinkel, K.M., Nelson, F.E., 2000. The Circumpolar Active Layer Monitoring (CALM) program: research designs and initial results. *Polar Geography*, 24 (3): 165-258.
- Global ecosystems database version 1.0 on CD-ROM. 1992. Series USDOC/NOAA National Geophysical Data Center, Boulder.
- Instanes, A., O. Anisimov, L. Brigham, D. Goering, B. Ladanyi, J.O. Larsen, and L.N. Khrustalev, 2005. Chapter 16: Infrastructure: Buildings, Support Systems, and Industrial Facilities. In: *Arctic Climate Impact Assessment, ACIA*. Cambridge: Cambridge University Press, , pp. 907-944.
- Intergovernmental panel on Climate Change (IPCC). 2007. *IPCC Working Group II Climate Change Impacts, Adaptation and Vulnerability Fourth Assessment Report, Chapter 15 Polar Regions (Arctic and Antarctic)*. www.ipcc.ch.
- Geo-Slope. 2007. Thermal modelling with TEMP/W 2007. An engineering methodology. Calgary, Canada: GEO-SLOPE International Ltd. 240 pages.
- Harris, C., D. Vonder Mühlh, K. Isaksen, W. Haerberli, J.L. Sollid, L. King, P. Holmlund, F. Dramis, M. Guglielmin, and D. Palacios, 2003: Warming permafrost in European mountains. *Global and Planetary Change*, 39, 215-225.
- Hinzman, L.D., N.D. Bettez, W. Bolton, R. F.S. Chapin III, M.B. Dyurgerov, C.L. Fastie, B. Griffith, R. Hollister, D. A. Hope, H. Huntington, A.M. Jensen, G.J. Jia, T. Jorgenson, D.L. Kane, D.R. Klein, G. Kofinas, A.H. Lynch, A.H. Lloyd, A.D. McGuire, F.E. Nelson, M. Nolan, W.C. Oechel, T.E. Osterkamp, C.H. Racine, V.E. Romanovsky, R.S. Stone, D.A. Stow, M. Sturm, C.E. Tweedie, G.L. Vourlitis, M.D. Walker, D.A. Walker, P.J. Webber, J. Welker, K.S. Winker, and K. Yoshikawa, 2005: Evidence and implications of recent climate change in northern Alaska and other arctic regions. *Climatic Change*, 72, 251-298.
- Khrustalev, L.N. 2001. Problems of permafrost engineering as related to global climate warming. In: R. Paep and V. Melnikov (eds.) *Permafrost Response on Economic Development, Environmental Security and Natural Resources*. Dordrecht, the Netherlands: Kluwer Academic Publishers, pp. 407-423.
- Nelson, F.E., Anisimov, O.A. and Shiklomanov, N.I., 2001. Subsidence risk from thawing permafrost. *Nature*, 410: 889-890.
- New, M., Hulme, M., Jones, P., 1999. Representing twentieth-century space-time climate variability. Part I: Development of a 1961-90 mean monthly terrestrial climatology. *Journal of Climate*, 12 (3): 829-856.

- McBean, G., G. Alekseev, D. Chen, E. Førland, J. Fyfe, P. Y. Groisman, R. King, H. Melling, R. Vose, and P. H. Whitfield, 2005: Chapter 2: Arctic Climate - Past and Present. *Arctic Climate Impacts Assessment (ACIA)*. C. Symon, L. Arris, B. Heal, Eds., Cambridge University Press, Cambridge, UK, 21-60.
- Romanovsky, V.E. and Osterkamp, T.E. 2001. Permafrost: Changes and impacts. In R. Paepe and V. Mel-nikov (eds.) *Permafrost Response on Economic Development, Environmental Security and Natural Resources*. Dordrecht, the Netherlands: Kluwer Academic Publishers, pp.297-315.
- Pavlov, A.V., and N.G. Moskalenko, 2002: The thermal regime of soils in the north of Western Siberia. *Permafrost Periglacial Process.*, **13**(1), 43-51.
- Romanovsky, V.E., M. Burgess, S. Smith, K. Yoshikawa, and J. Brown, 2002: Permafrost temperature records: Indicators of climate change. *EOS, Transactions, American Geophysical Union*, 83, 589-594.
- Sazonova, T.S., Romanovsky, V.E., 2003. A model for regional-scale estimation of temporal and spatial variability of active-layer thickness and mean annual ground temperatures. *Permafrost and Periglacial Processes*, 14 (2): 125- 140.
- Symon, C. (Editor), 2005. *Impacts of a Warming Arctic: Arctic Climate Impacts Assessment*. Cambridge University Press, Cambridge, 1042 pp.
- Vasilieva, I., 2004: *Climate, thawing permafrost, and buildings in the Northern lands. Expert - 9 Siberia*. Yakutsk, pp. 2nd October 2004.
- Zernova, L. 2003. *Has the frost cancelled the predicted global warming? The City*. St. Petersburg, Russia, pp. 14-15.

Table 1. Maximum ground temperature along the embedded pile length for each decade, Fairbanks, Alaska

Depth (m)	1929 (°C)	1931 (°C)	1942 (°C)	1953 (°C)	1963 (°C)	1978 (°C)	1987 (°C)	1994 (°C)	2003 (°C)
1	+5.99	+5.54	+5.41	+5.31	+5.42	+6.30	+6.69	+6.39	+7.66
2	-1.00	-1.36	-1.09	-1.25	-1.24	-1.11	-0.92	-0.71	-0.89
3	-2.07	-2.19	-2.07	-2.15	-2.18	-2.02	-1.96	-1.93	-1.98
4	-2.44	-2.71	-2.70	-2.75	-2.87	-2.63	-2.48	-2.48	-2.43
5	-2.91	-3.18	-3.20	-3.34	-3.49	-3.20	-2.97	-2.96	-2.89
6	-3.34	-3.63	-3.65	-3.88	-4.04	-3.63	-3.42	-3.37	-3.26
7	-3.73	-4.02	-4.03	-4.37	-4.53	-4.04	-3.73	-3.76	-3.60
8	-4.04	-4.36	-4.39	-4.80	-4.92	-4.42	-4.05	-4.08	-3.91
9	-4.28	-4.57	-4.71	-5.04	-5.20	-4.74	-4.33	-4.32	-4.18
10	-4.51	-4.74	-4.91	-5.30	-5.44	-4.95	-4.58	-4.55	-4.36
11	-4.70	-4.92	-5.08	-5.52	-5.63	-5.16	-4.70	-4.72	-4.53
12	-4.84	-5.01	-5.24	-5.67	-5.78	-5.33	-4.81	-4.84	-4.68

Table 2. Maximum ground temperature along the embedded pile length for each decade, Longyearbyen, Norway

Depth (m)	1926 (°C)	1939 (°C)	1941 (°C)	1958 (°C)	1961 (°C)	1977 (°C)	1986 (°C)	2000 (°C)	2007 (°C)
1	-1.30	-1.25	-1.50	-1.30	-1.23	-1.43	-1.36	-1.08	-0.08
2	-2.40	-2.20	-2.49	-2.18	-2.27	-2.38	-2.34	-2.30	-1.86
3	-3.26	-2.77	-3.28	-2.84	-3.01	-3.20	-3.14	-2.98	-2.30
4	-3.96	-3.33	-3.88	-3.38	-3.68	-3.91	-3.80	-3.63	-2.85
5	-4.53	-3.75	-4.32	-3.85	-4.24	-4.55	-4.37	-4.23	-3.10
6	-5.02	-4.12	-4.76	-4.30	-4.60	-5.13	-4.83	-4.64	-3.40
7	-5.48	-4.46	-5.09	-4.71	-4.96	-5.48	-5.25	-5.03	-3.70
8	-5.76	-4.73	-5.29	-5.00	-5.24	-5.82	-5.56	-5.34	-3.98
9	-6.03	-4.94	-5.49	-5.23	-5.44	-6.05	-5.81	-5.60	-4.18
10	-6.24	-5.13	-5.59	-5.45	-5.64	-6.25	-6.00	-5.81	-4.38
11	-6.39	-5.27	-5.68	-5.60	-5.75	-6.40	-6.15	-5.98	-4.53
12	-6.53	-5.39	-5.74	-5.74	-5.87	-6.52	-6.28	-6.11	-4.67

Table 3. Maximum ground temperature along the embedded pile length for each decade, Yakutsk, Russia

Depth (m)	1920 (°C)	1934 (°C)	1949 (°C)	1950 (°C)	1966 (°C)	1976 (°C)	1989 (°C)	1997 (°C)	2002 (°C)
1	+4.89	+5.16	+5.36	+5.22	+4.80	+6.02	+5.15	+5.94	+5.95
2	-1.89	-1.88	-1.84	-1.97	-1.92	-1.93	-1.87	-1.65	-1.56
3	-3.45	-3.43	-3.46	-3.65	-3.51	-3.48	-3.51	-3.25	-3.19
4	-4.95	-4.93	-5.02	-5.23	-5.04	-5.00	-4.94	-4.62	-4.54
5	-6.19	-6.33	-6.38	-6.72	-6.47	-6.42	-6.29	-5.91	-5.82
6	-7.36	-7.60	-7.50	-8.04	-7.75	-7.69	-7.50	-7.04	-6.99
7	-8.37	-8.50	-8.50	-9.06	-8.57	-8.67	-8.37	-7.80	-7.81
8	-9.18	-9.26	-9.38	-9.89	-9.38	-9.38	-9.10	-8.54	-8.52
9	-9.80	-9.98	-10.10	-10.54	-10.12	-10.08	-9.80	-9.22	-9.19
10	-10.35	-10.47	-10.58	-11.03	-10.58	-10.59	-10.27	-9.61	-9.64
11	-10.76	-10.88	-11.00	-11.41	-11.02	-10.98	-10.68	-10.00	-10.03
12	-11.10	-11.23	-11.33	-11.67	-11.35	-11.33	-11.02	-10.30	-10.36